© 2019. Published by The Company of Biologists Ltd | Journal of Cell Science (2019) 132, jcs224147. doi:10.1242/jcs.224147

RESEARCH ARTICLE

Dual role for fungal-specific outer kinetochore proteins during cell cycle and development in *Magnaporthe oryzae*

Hiral Shah[1], Kanika Rawat[1,*,§], Harsh Ashar[1,‡,§], Rajesh Patkar[1,¶] and Johannes Manjrekar[2,¶]

ABSTRACT

The outer kinetochore DASH complex (also known as the Dam1 complex) ensures proper spindle structure and chromosome segregation. While DASH complex protein requirement diverges among different yeasts, its role in filamentous fungi has not yet been investigated. We studied the dynamics and role of middle (Mis12) and outer (Dam1 and Ask1) kinetochore proteins in the filamentous fungal pathogen, *Magnaporthe oryzae*, which undergoes multiple cell cycle-linked developmental transitions. While Mis12 was constitutively present in the nucleus, Dam1 and Ask1 were recruited only during mitosis. Although Dam1 was not required for viability, loss of its function (*dam1*Δ) delayed mitotic progression, resulting in impaired conidial and hyphal development. Both Dam1 and Ask1 also localised to the hyphal tips, in the form of punctae oscillating back and forth from the growing ends, suggesting that *Magnaporthe* DASH complex proteins may play a non-canonical role in polarised growth during interphase, in addition to their function in nuclear segregation during mitosis. Impaired appressorial (infection structure) development and host penetration in the *dam1*Δ mutant suggest that fungus-specific Dam1 complex proteins could be an attractive target for a novel anti-fungal strategy.

This article has an associated First Person interview with the first author of the paper.

KEY WORDS: Kinetochore, Dam1 complex, DASH complex, Filamentous fungus, *Magnaporthe*, Rice blast fungus

INTRODUCTION

Chromosome segregation is a determining step in cell division. During mitosis, the kinetochore (KT) brings about precise chromosome segregation at anaphase and anomalies in chromosome separation are associated with malfunction and disease in multicellular organisms. In unicellular yeasts, such aberrant chromosomal segregation often leads to loss of viability. The kinetochore differs in structure and composition among eukaryotes (Van Hooff et al., 2017). The microtubule (MT)-associated DASH complex (also known as the Dam1 complex) is a fungus-specific component of the outer kinetochore. This complex has varying roles in the yeasts *Saccharomyces cerevisiae*, *Schizosaccharomyes pombe* and *Candida albicans*, where it has been studied extensively; however, very little is known about its function in filamentous fungi.

The DASH complex is made up of 10 subunits, namely Dam1, Ask1, Spc34, Hsk3, Dad1–Dad4, Duo1 and Spc19, all of which are essential for viability in *S. cerevisiae* and *C. albicans*. By contrast, none of these subunits are individually essential for survival in *S. pombe*. In *S. cerevisiae*, Dam1 is required for proper spindle assembly and elongation (Hofmann et al., 1998; Cheeseman et al., 2001a), while Ask1 is required for bipolar attachment (Janke et al., 2002). Dam1 directly interacts with MTs and other DASH members to form DASH complex oligomers (Legal et al., 2016). The yeast DASH complex members are MT plus-end-interacting proteins (TIPs). The *S. pombe dam1*Δ mutant displays chromosome segregation delay and ectopic septation (Sanchez-Perez et al., 2005). Further, *S. pombe* DASH complex mutants are sensitive to the MT poison thiabendazole, low temperature and high osmolarity – all phenotypes shared by genes involved in MT stability and dynamics (Sanchez-Perez et al., 2005; Gao et al., 2010). Dam1 was also discovered to be a multicopy suppressor of mutations in the spindle regulator Cdc13, and MT plus-end-binding protein Mal3 (Eb1 in mammalian cells) (Sanchez-Perez et al., 2005). Further, in *S. pombe*, retrieval of unclustered kinetochores is dependent on Dam1 (Franco et al., 2007).

In *S. pombe*, Dam1 is recruited to the kinetochore in early mitosis, where it is observed as a single spot that resolves into several spots at metaphase, while Dad1 remains associated with the kinetochore throughout the cell cycle (Liu et al., 2005; Sanchez-Perez et al., 2005). The DASH complex spots co-localise with other kinetochore proteins such as Mtw1 (in *S. cerevisiae*; Mis12 in *S. pombe*) and Ndc80 (Sanchez-Perez et al., 2005). In *S. cerevisiae*, Dam1 is present at the kinetochore throughout the cell cycle, clustered as a single nucleus-associated spot during interphase, which divides into two spots closely associated with the spindle pole bodies at mitosis. Dam1 has also been observed all along the spindle in *S. cerevisiae*. Association of Ask1 with the kinetochore is dependent on Ndc10 (also known as Cbf2 in *S. cerevisiae*) and the MT spindle in budding yeast. *In vitro* MT-binding studies using *S. cerevisiae* proteins have shown 16-member oligomeric rings that encircle the MT. However, rings are not essential for MT attachment. Recently, electron cryotomography studies in *S. cerevisiae* cells have shown the presence of one or two, partial or complete rings with 17-fold symmetry associated with spindle MTs (Ng et al., 2019).

With respect to nuclear envelope continuity, fungi exhibit a spectrum of types of mitosis. While *S. cerevisiae* and *S. pombe* both undergo closed mitosis, filamentous fungi show differences; semi-open in *Aspergillus nidulans*, open in *Ustilago maydis* and semi-closed in *Magnaporthe oryzae*. Further, in *S. cerevisiae* mitosis lasts around 50 min while in *S. pombe* and many filamentous fungi it

[1]Bharat Chattoo Genome Research Centre, Department of Microbiology and Biotechnology Centre, The Maharaja Sayajirao University of Baroda, Vadodara 390002, Gujarat, India. [2]Biotechnology Programme, Department of Microbiology and Biotechnology Centre, The Maharaja Sayajirao University of Baroda, Vadodara 390002, Gujarat, India.
*Present address: Centre for Ecological Sciences, Indian Institute of Science, Bengaluru-560012, Karnataka, India. ‡Present address: Stem Cell Biology Group, Advanced Centre for Treatment, Research and Education in Cancer, Tata Memorial Centre, Kharghar, Navi Mumbai 410210, Maharashtra, India.
§These authors contributed equally to this work

¶Authors for correspondence (jmanjrekar@yahoo.com; rajeshpatkar-biotech@msubaroda.ac.in)

H.S., 0000-0002-8143-8244; K.R., 0000-0002-8309-7754; H.A., 0000-0003-2140-8542; R.P., 0000-0001-7266-2394; J.M., 0000-0001-8760-2028

Received 25 August 2018; Accepted 7 May 2019

Journal of Cell Science (2019) 132, jcs224147. doi:10.1242/jcs.224147

is completed in less than 5 min. In addition, mitosis in filamentous fungi is often associated with distinct morphological differentiation not observed in most yeasts, setting different requirements and constraints on spindle assembly and elongation. Thus, owing to these differences, it is likely that KT–spindle structure and assembly differ in filamentous fungi. Unlike yeasts, the filamentous fungal pathogen *M. oryzae* undergoes several morphologically distinct developmental transitions during its life cycle.

During the *M. oryzae* pathogenic life cycle, the three-celled conidium germinates on the leaf surface to extend a polarised germ tube. While entry of the germinating cell nucleus into S phase is required for the swelling of the germ tube tip (switching from polarised to isotropic growth to form the incipient appressorium), entry into mitosis is necessary for the further development of the appressorium (Saunders et al., 2010a). The diploid nucleus of the germinating cell undergoes the first round of infection-related mitosis in the germ tube. Nuclear division is followed by migration, during which one daughter nucleus returns to the germinated cell in the conidium and the other travels into the appressorium. Subsequently, exit from mitosis is required for appressorium maturation and function (Saunders et al., 2010b). Interestingly, the appressorium then switches back to polarised growth to form the penetration peg that breaches the host epidermis and elaborates into the primary infection hypha (IH). This developmental transition is again dependent on the S phase checkpoint. At this point, the second round of infection-related mitosis in the mature appressorium contributes a nucleus to the IH. The IH nuclei undergo semi-closed mitosis lasting roughly 3 min (Jones et al., 2016). Thus, the crucial morphological transitions during *M. oryzae* infection are tightly coupled to different stages of the cell cycle. Secondary hyphae then develop from the primary IH and spread to the neighbouring host cells, resulting in typical disease lesions in a few days. These secondary hyphae later give rise to the aerial hyphae, some of which eventually form conidiophores bearing 3–5 sympodial conidia. A single lesion can produce a new generation of thousands of conidia that can initiate a new infection cycle.

M. oryzae infects rice and several other cereal crops across the world, and is a serious threat to global food security (Dean et al., 2012). Investigating the role of fungus-specific components in the development of this fungus would provide new targets for novel anti-fungal strategies. DASH complex proteins are not found in rice or other plant hosts making them potential candidates; however, within filamentous fungi, only the Duo1 subunit of *Magnaporthe* has been studied so far. The *M. oryzae* protein Duo1 plays a role in conidiation and full virulence in rice, but not much information is available regarding its function as a kinetochore protein in mitosis or its localisation during the cell cycle (Peng et al., 2011). In this study, we focused on the role of DASH complex proteins in chromosome segregation, especially during the cell cycle-regulated morphological transitions in *M. oryzae.* Using deletion mutants and GFP-tagged strains, we studied the behaviour of Dam1 and Ask1 during nuclear division, spindle dynamics and nuclear migration, and its effect on *M. oryzae* development. We show that in addition to its role in proper chromosome segregation, Dam1 – through its localisation in the hyphal tip compartment during interphase – is involved in polarised growth.

RESULTS

DASH complex protein Dam1 is recruited to the nucleus during mitosis

We identified the orthologue of *S. cerevisiae* and *S. pombe* Dam1 in *M. oryzae* (MGG_00874) using BLASTP. Although the overall protein sequence similarity was ∼30–40%, the DASH complex domain of *M. oryzae* Dam1 showed significant homology (∼60%) with that of yeasts. The Dam1 proteins show considerable size variation across organisms, ranging from 343 amino acids in *S. cerevisiae* to 121 in *Cryptococcus neoformans*, with the *M. oryzae* protein being 220 amino acids (Table S1). The protein size variation is mainly due to differences in the length of the C-terminal region. We further identified another member of the DASH complex in *M. oryzae*, Ask1 (MGG_07143), which is known to directly interact with Dam1 in *S. cerevisiae*. To study the subcellular localisation and dynamics of these proteins in relation to those of the nucleus, we tagged Dam1 and Ask1, separately, with GFP in a strain expressing histone H1–mCherry (hH1–mCherry). As a marker for kinetochore position, we also studied the localisation of the middle kinetochore MIND complex protein Mis12 (MGG_06304) in *Magnaporthe*.

In vegetative hyphae, Mis12–GFP was observed as a single distinct puncta at the periphery of the interphase nucleus (arrowhead, Fig. 1A). In contrast, the DASH complex proteins GFP–Dam1 and Ask1–GFP did not localise predominantly to the nucleus during interphase (Fig. 1A). Occasionally, non-nuclear GFP–Dam1 or Ask1–GFP punctae were seen along the hyphae (arrows, Fig. 1A). We presumed these were DASH complex proteins associated with cytoplasmic MTs. At the onset of mitosis (marked by chromosome condensation), while the Mis12–GFP de-clustered, the GFP–Dam1 punctae appeared at the nucleus and persisted there throughout the mitotic process and the subsequent nuclear migration (arrowheads, Fig. 1B). At the end of mitosis, the Mis12–GFP and GFP–Dam1 spots re-clustered into a single spot per nucleus (Fig. 1B). To determine whether DASH complex proteins had similar dynamics during the early infection process of *M. oryzae*, we studied GFP–Dam1 and Ask1–GFP localisation during appressorium formation. The Ask1–GFP and GFP–Dam1 punctae were associated with the nucleus during nuclear division and migration in the course of appressorial development (lower panels, Fig. 1C; Fig. S1). Thus, while the middle kinetochore layer protein Mis12 was constitutively associated with the *M. oryzae* kinetochore, the outer layer DASH complex proteins were recruited to the nucleus specifically during mitosis.

Dam1 plays an important role in proper segregation of chromosomes

We monitored the dynamics of nuclei marked with hH1–mCherry and MTs or spindle marked with GFP (β tubulin–sGFP, Tub–GFP hereafter) during mitosis in vegetative hyphae of *M. oryzae*. Concurrently, to investigate the role of DASH complex proteins in mitosis, we generated *DAM1* deletion (*dam1*Δ) strains in the wild-type (WT) and the strain expressing hH1–mCherry and Tub–GFP. Additionally, we deleted *ASK1* (*ask1*Δ) in a strain expressing GFP–Dam1. At the onset of mitosis in the WT strain, prophase was marked by MT re-organisation and chromosome condensation. It was characterised by the loss of cytoplasmic MT arrays and establishment of a single tubulin focal point at the nucleus, which is probably a site for spindle MT nucleation. This was followed by the assembly of an intensely fluorescent bipolar spindle, which underwent re-orientation to align along the long axis of the hypha. Once formed, the spindle length remained largely constant until its elongation during anaphase. The chromosomes then segregated into two daughter nuclei that migrated to opposite ends (Fig. 2A). The *dam1*Δ strain showed longer spindles (5.37±0.16 µm) when compared to the WT (3.71±0.07 µm) (mean±s.e.m.) (Fig. 2B). We further determined the time for which the spindle

Journal of Cell Science (2019) 132, jcs224147. doi:10.1242/jcs.224147

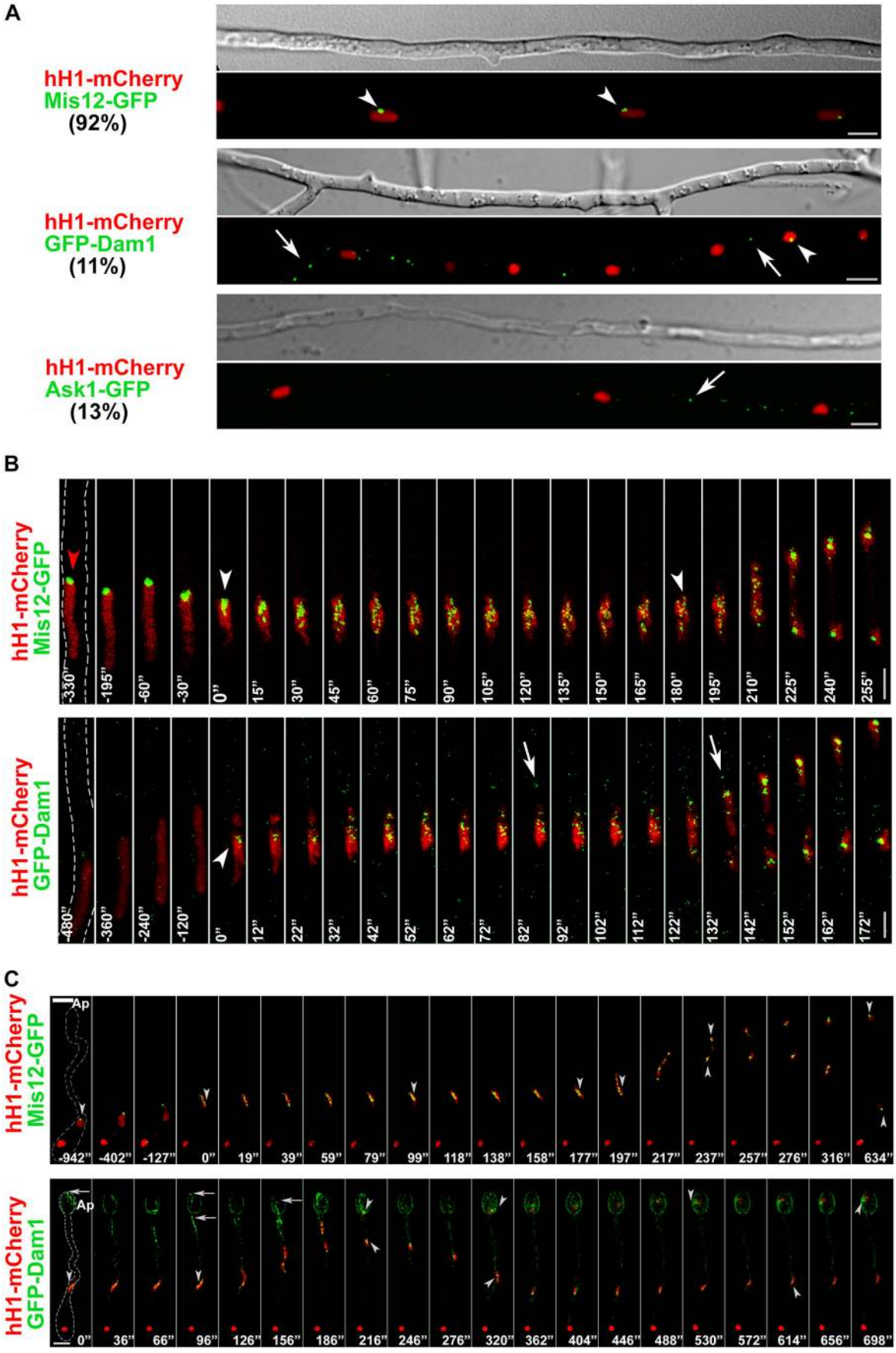

Fig. 1. See next page for legend.

Fig. 1. Dam1 is recruited to the nucleus at the onset of mitosis. (A) Localisation of middle (Mis12–GFP, *n*=207) and outer (GFP–Dam1, *n*=207 and Ask1–GFP, *n*=227) kinetochore proteins during interphase in vegetative hyphae. Numbers indicate percentage of nuclei with associated KT proteins during interphase. Arrowheads indicate nuclear-associated Mis12–GFP or GFP–Dam1. Arrows denote GFP–Dam1 or Ask1–GFP spots probably associated with cytoplasmic MTs. Scale bars: 5 µm. (B) Time-lapse images showing dynamics of Mis12–GFP and GFP–Dam1 during mitosis in vegetative hyphae, *n*=10. Numbers indicate time in seconds. Fungal structures are marked with dashed outlines. Arrowheads indicate nuclear-associated Mis12–GFP or GFP–Dam1. Red arrowhead indicates Mis12–GFP associated with the nucleus prior to mitosis. Arrows denote GFP–Dam1 spots probably associated with cytoplasmic MTs along the vegetative hyphae. Scale bars: 3 µm. (C) Localisation of middle (Mis12–GFP) and outer (GFP–Dam1) kinetochore proteins during appressorium (Ap) development, *n*=5. Numbers indicate time in seconds. Fungal structures are indicated as dashed outlines. Arrowheads indicate nuclear-associated Mis12–GFP or GFP–Dam1. Arrows indicate non-nuclear spots of GFP–Dam1 in appressorium. Scale bar: 5 µm.

persisted until the onset of anaphase in the WT and *dam1*Δ strains. The *dam1*Δ mutant showed a significant delay in spindle elongation compared to the WT (Fig. 2C). While chromosome segregation was mostly initiated within 3 min in the WT (2.31±0.15 min), anaphase onset in several *dam1*Δ mutant cells took more than 10 min (8.70±1.29 min) (Fig. 2C,D). The time spent in metaphase or prior to anaphase varied considerably between individual cells in the *dam1*Δ strain (3–39 min) (Fig. 2D). The duration of mitosis in the germ tube during appressorium development showed a similar delay in the *dam1*Δ mutant (Fig. 2E). Importantly, in a few *dam1*Δ cells, we occasionally observed unequal segregation of nuclear material or lagging chromosomes that moved behind the rest (arrows, Fig. 2C). Thus, Dam1 function probably ensures correct spindle structure and separation of chromosomes at anaphase, allowing proper mitotic progression during both vegetative (hyphal) growth and pathogenic (appressorial) development in *M. oryzae*.

The DASH complex is involved in polarised hyphal growth

Next, we looked at the effects of delayed mitosis resulting from the loss of Dam1 or Ask1 function. We found that the *dam1*Δ (Fig. 3A) and *ask1*Δ (Fig. S2A) strains had a significantly reduced colony diameter, mainly due to aberrant vegetative hyphal extension and morphology. Radial hyphal growth (in terms of colony diameter) was restored in the complementation strain *dam1*Δ/*DAM1* (Fig. 3A). In *M. oryzae*, hyphae grow by apical extension and lateral branching. The branches arose close to the septa at acute angles to the growing primary hypha and at fairly regular intervals in the WT. The hyphae of the *dam1*Δ strain showed a zigzag or curved morphology, unlike the mostly straight hyphae of the WT, and showed more frequent branching (Fig. 3B,C; Fig. S3A). The *dam1*Δ mutants also showed a higher number of branches emerging at angles >60° compared to WT (Fig. S3B,C). Since branching is often associated with septation, we asked whether there was a change in cell size upon loss of Dam1 function in *M. oryzae*. Indeed, Calcofluor White (CFW) staining of the *dam1*Δ hyphae showed smaller sub-apical cell compartments compared to the WT (Fig. 3D,E). A similar septation defect was seen in the vegetative hyphae of the *ask1*Δ mutant (Fig. S2D). Septation probably leads to branching by acting as a barrier to movement of growth proteins and exocytic vesicles towards the tip, leading to their accumulation.

Interestingly, we observed that GFP–Dam1 localises to the hyphal tip in the form of distinct spots during interphase (Fig. 4A). These intense spots were highly dynamic, and moved forward with the growing tips (Fig. 4B). To check whether this non-conventional localisation during interphase was specific to Dam1 or involved the DASH complex, we also studied Ask1–GFP localisation. Indeed, Ask1–GFP also localised to the growing hyphal tips in a similar manner. Further, intriguingly, Ask1–GFP (Fig. 4C) and GFP–Dam1 (Fig. 4D) spots showed an oscillatory movement to the tip and back towards the nucleus, suggesting their movement along long tracks. Another stage of the *M. oryzae* life cycle that involves polarised growth is the extension of the germ tube during the early stage of pathogenic development. Dynamic Ask1–GFP and GFP–Dam1 spots, similar to the ones seen in the hyphal tip, were observed at the tips of the germ tubes, suggesting a role for the DASH complex in polarised growth during pathogenic development in *M. oryzae* (Fig. 4E).

We next asked whether the observed localisation and dynamics of Dam1 required the MT network. Upon treatment with the MT-destabilising compound nocodazole, the dynamic GFP–Dam1 punctae became static aggregates, randomly distributed along the germ tube cytoplasm (Fig. 4F). Thus, the MT-based oscillatory behaviour of Dam1 suggests a non-canonical function for this DASH complex protein prior to the onset of mitosis, and that the growth defects seen in the *dam1*Δ strain are a combined outcome of delayed mitosis and impaired polarised growth upon loss of Dam1 function in *Magnaporthe*.

Conidiogenesis is marked by three distinct rounds of mitosis

Production of three-celled conidia is a critical developmental step in the life cycle of *M. oryzae*. However, the mitotic events and cell cycle regulation involved in conidial development have not been studied in any detail to date. We first monitored mitosis during conidium development in the strain expressing hH1–mCherry and Tub–GFP. Development of the three-celled conidium takes 5–7 h, with extremely short mitosis events separated by 1.5–2.5 h interphases characterised by cell growth. It has already been shown that conidial development starts with the shift from polarised to isotropic growth, where the tip of the aerial hypha starts swelling to form an incipient conidium (conidiophore) (Deng et al., 2009). We found that the first nuclear division took place in the stalk and was followed by nuclear migration where one of the daughter nuclei travelled into the conidium cell (mitosis I, Fig. 5A) while the other remained in the stalk. This was followed by cytokinesis (septation), which probably occurred at the neck of the incipient conidium, away from the site of mitosis in the stalk. This spatial uncoupling of cytokinesis from mitosis was similar to the events observed during appressorium development, and different from what was observed in vegetative hyphal growth. The single-celled conidium then grew and elongated into an oval-shaped cell with the nucleus positioned close to the centre. This nucleus underwent division, with one of the daughter nuclei remaining positioned at the base (towards the stalk) of the conidium and the other moving to the opposite end. The process was accompanied by active re-organisation of the MT network and septation at the site of mitosis to form an intermediate two-celled conidium (asterisk, mitosis II, Fig. 5A). Subsequently, the nucleus in the second cell of the developing conidium underwent the third round of division, followed by cytokinesis to form the middle and terminal cells of the mature three-celled conidium (mitosis III, Fig. 5B).

We next studied the localisation of GFP–Dam1 during mitoses in the developing conidia. We observed that GFP–Dam1 localised to the nucleus during all three rounds of nuclear division during conidiation (Fig. 5B). It appeared in the form of multiple spots during mitosis, and then clustered into two distinct spots, one per nucleus, and persisted until nuclear migration and positioning was complete. As in the case of vegetative hyphae, GFP–Dam1 or

Journal of Cell Science (2019) 132, jcs224147. doi:10.1242/jcs.224147

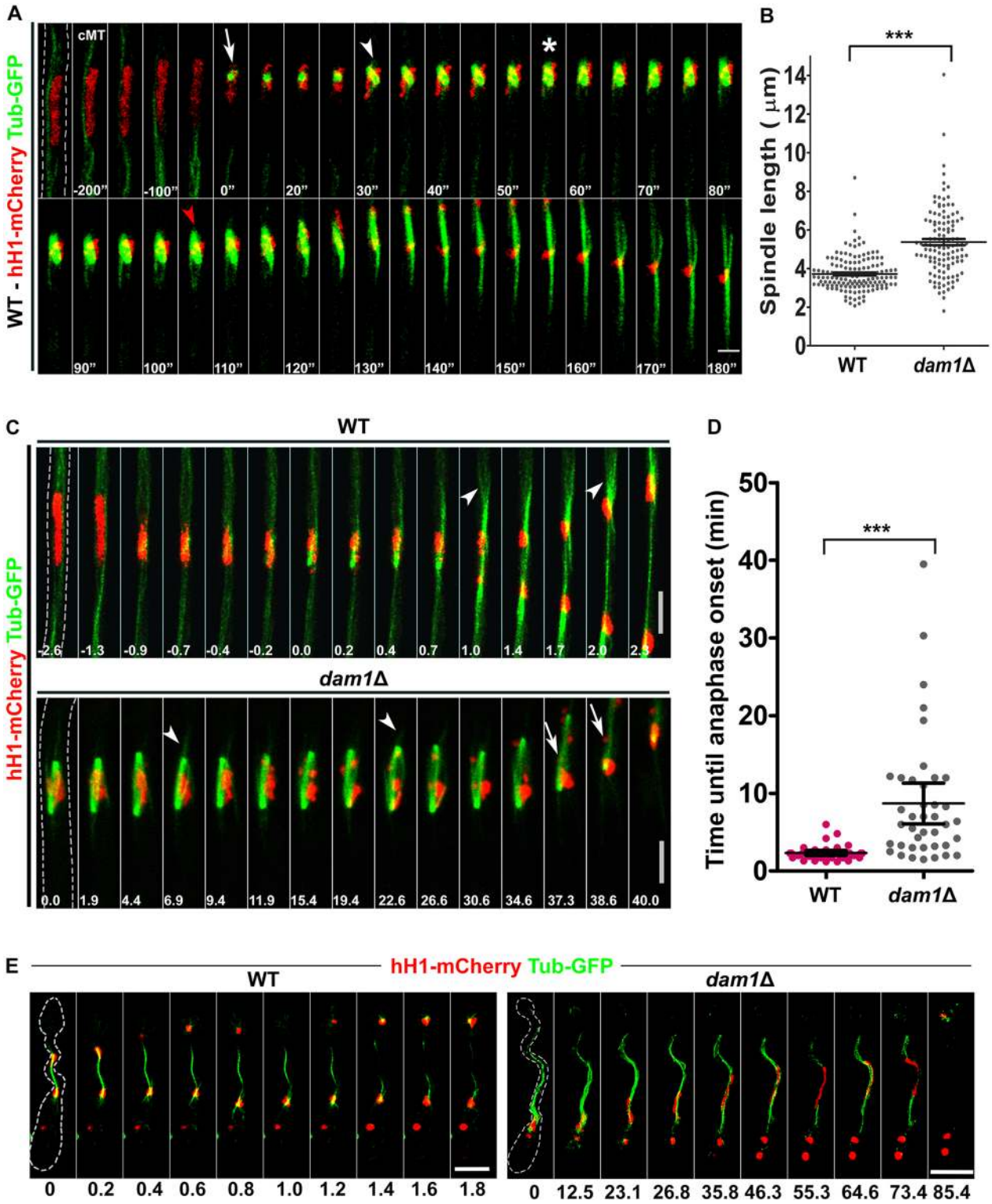

Fig. 2. Dam1 plays an important role in proper segregation of chromosomes during nuclear division. (A) Dynamics of the mitotic spindle in WT *M. oryzae* expressing Tub–GFP and hH1–mCherry. Numbers indicate time in minutes. Hyphal borders are indicated with dashed lines. Arrow depicts entry into mitosis, arrowhead indicates assembly of a bipolar spindle, asterisk shows spindle re-orientation, and red arrowhead indicates onset of spindle elongation. Scale bar: 3 µm. cMT, cytoplasmic MTs. (B) Scatter plot showing mean±s.e.m. spindle length in the WT (n=143) and *dam1*Δ (n=119) strains during mitosis. ***P<0.001, two-tailed t-test. (C) Time-lapse images of mitosis in WT and *dam1*Δ vegetative hyphae. Numbers indicate time in minutes. Hyphae are marked with dashed outlines. Arrowheads indicate astral MTs and arrows show lagging chromosomes. Scale bars: 5 µm. (D) Scatter plot showing mean±s.e.m. time until spindle elongation in anaphase in WT and *dam1*Δ strains during mitosis in vegetative hyphae. ***P<0.001, two-tailed t-test, n=40. (E) Time-lapse images of mitosis during appressorium development in the WT and *dam1*Δ strain. Numbers indicate time in minutes. Fungal structures are marked with dashed outlines. Scale bars: 10 µm.

Journal of Cell Science (2019) 132, jcs224147. doi:10.1242/jcs.224147

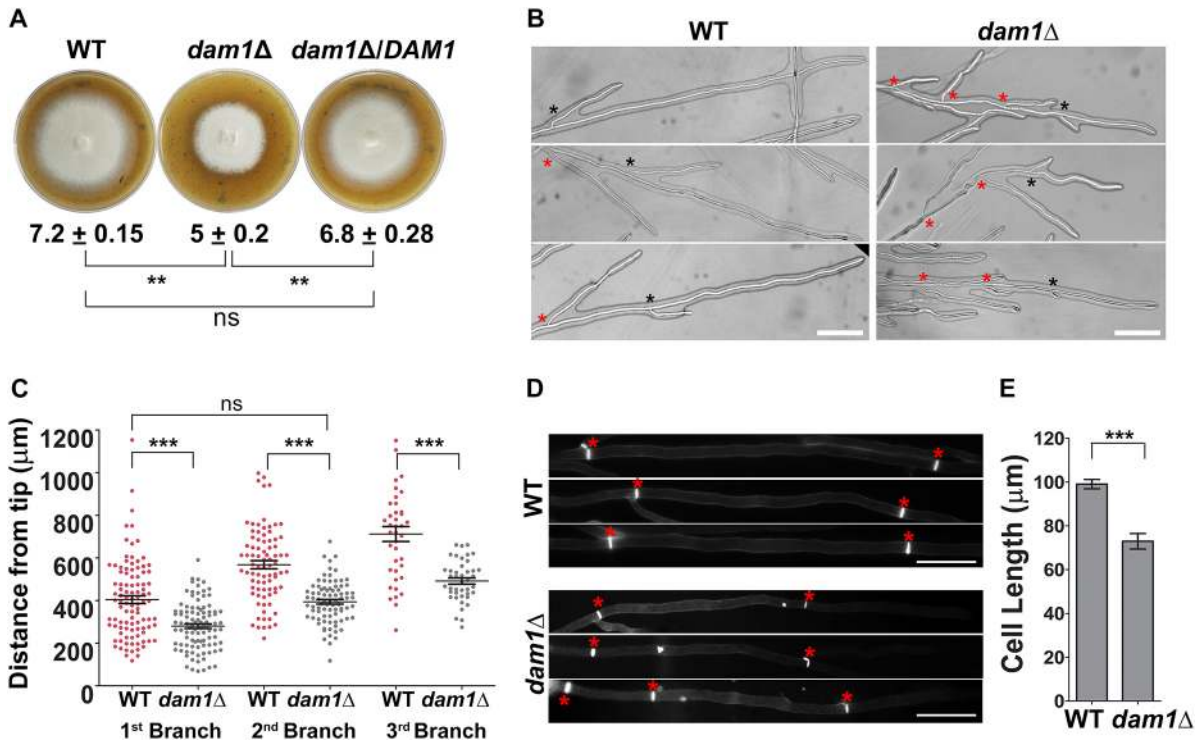

Fig. 3. The DASH complex is involved in polarised hyphal growth. (A) Vegetative growth of WT, *dam1*Δ and *dam1*Δ/*DAM1* strains at 10 dpi on prune agar. Numbers indicate mean±s.e.m. colony diameter in centimetres from three independent experiments with n=3 each. **P<0.05; ns, not significantly different; two-tailed t-test. (B) Difference in the branching pattern of vegetative hyphae in the WT and *dam1*Δ strain. Black asterisks indicates first branch from the tip. Red asterisks indicate all subsequent branches. Scale bars: 100 µm. (C) Scatter plot showing mean±s.e.m. distance of first (n=100), second (n=80) and third branch (n=40) from the apical tip in the WT and *dam1*Δ vegetative hyphae from three independent experiments. ***P<0.001; ns, not significantly different, two-tailed t-test. (D) Sub-apical cell compartment length in WT and *dam1*Δ vegetative hyphae stained with Calcofluor White (CFW). Red asterisks indicate septa (cell boundaries). Scale bars: 20 µm. (E) Bar chart showing mean±s.e.m. length of sub-apical cell compartments in WT and *dam1*Δ vegetative hyphae from three independent experiments. ***P<0.0001, two-tailed t-test, n=200.

Ask1–GFP did not associate with the nucleus during the intermittent interphases. Occasionally, a cytoplasmic spot was seen during the initial conidiophore development prior to the first round of mitosis. Thus, Dam1 function plays a key role in three sequential and essential rounds of mitosis to form a complete three-celled asexual conidium.

Dam1 function is crucial for proper conidiation

In addition to reduced radial vegetative growth, the *dam1*Δ strain showed flat and white colonies, in contrast to the fluffy, grey growth of the WT, suggesting defects in the development of aerial hyphae that give rise to conidia. To assess the role of Dam1 protein during asexual conidium development, we studied the growth and morphology of the aerial hyphae and conidiophores in the *dam1*Δ strain. Most of the conidiophores of the *dam1*Δ strain bore only 1–3 conidia as compared to the sympodial cluster of 3–5 conidia observed in the WT (Fig. 6A,B) after 24 h of photo-induction. The total number of conidia in the *dam1*Δ strain was reduced to 10% of the WT, and the mutant conidia were smaller (14.61±0.12 µm) in length than those in the WT (23.05±0.47 µm) (mean±s.e.m. from three independent experiments with n=100 conidia). In addition, the *dam1*Δ mutant showed aberrant morphology compared to the WT when stained with CFW. In contrast to the three-celled pyriform conidia seen in the WT, *dam1*Δ mostly produced one- or two-celled oval conidia (Fig. 6C,D). The WT conidium morphology and cell number were restored in the complementation strain *dam1*Δ/*DAM1*, expressing the full-length Dam1 protein (Fig. 6D; Fig. S4D). The *ask1*Δ mutant displayed similar defects in the total conidium number and morphology (Fig. S2B,C). The WT three-celled conidia showed distinct cell boundaries with one nucleus per cell and a prominent MT network, especially along the septa, probably arising from septal microtubule organising centres (MTOCs). We further found that ∼50% of the *dam1*Δ conidia had aberrant nuclear and collapsed microtubular structures when compared to the WT (Fig. 6E,F). We infer that Dam1 function is required to ensure precise and orderly mitotic progression for proper conidial development and morphology in *M. oryzae*.

Dam1 function is required for proper pathogenic development and virulence

We studied infection-related (appressorial) development in the *dam1*Δ strain, to assess the role of Dam1 in pathogenesis of *M. oryzae*. In *in vitro* assays, the majority of the *dam1*Δ conidia failed to germinate (Fig. 7A). While 81% of the WT conidia formed appressoria, only 15% of the *dam1*Δ mutant conidia formed the infection structure (Fig. 7A,B). A few mutant conidia developed aberrant germ tubes and/or appressoria (Fig. 7A,C), when compared to the WT or the *dam1*Δ/*DAM1* complementation strain, which showed a single, short, non-septate germ tube giving rise to a mature and functional appressorium (Fig. S4E). While 83% of the WT appressoria could penetrate and colonise the rice leaf sheath tissue 40 h post inoculation, only 28% of the *dam1*Δ cells could do so (Fig. 7D,E). Next, we examined the virulence of the WT and *dam1*Δ mutant strains on susceptible CO-39 seedlings using a standard whole-plant infection assay. While the WT strain developed typical

Journal of Cell Science (2019) 132, jcs224147. doi:10.1242/jcs.224147

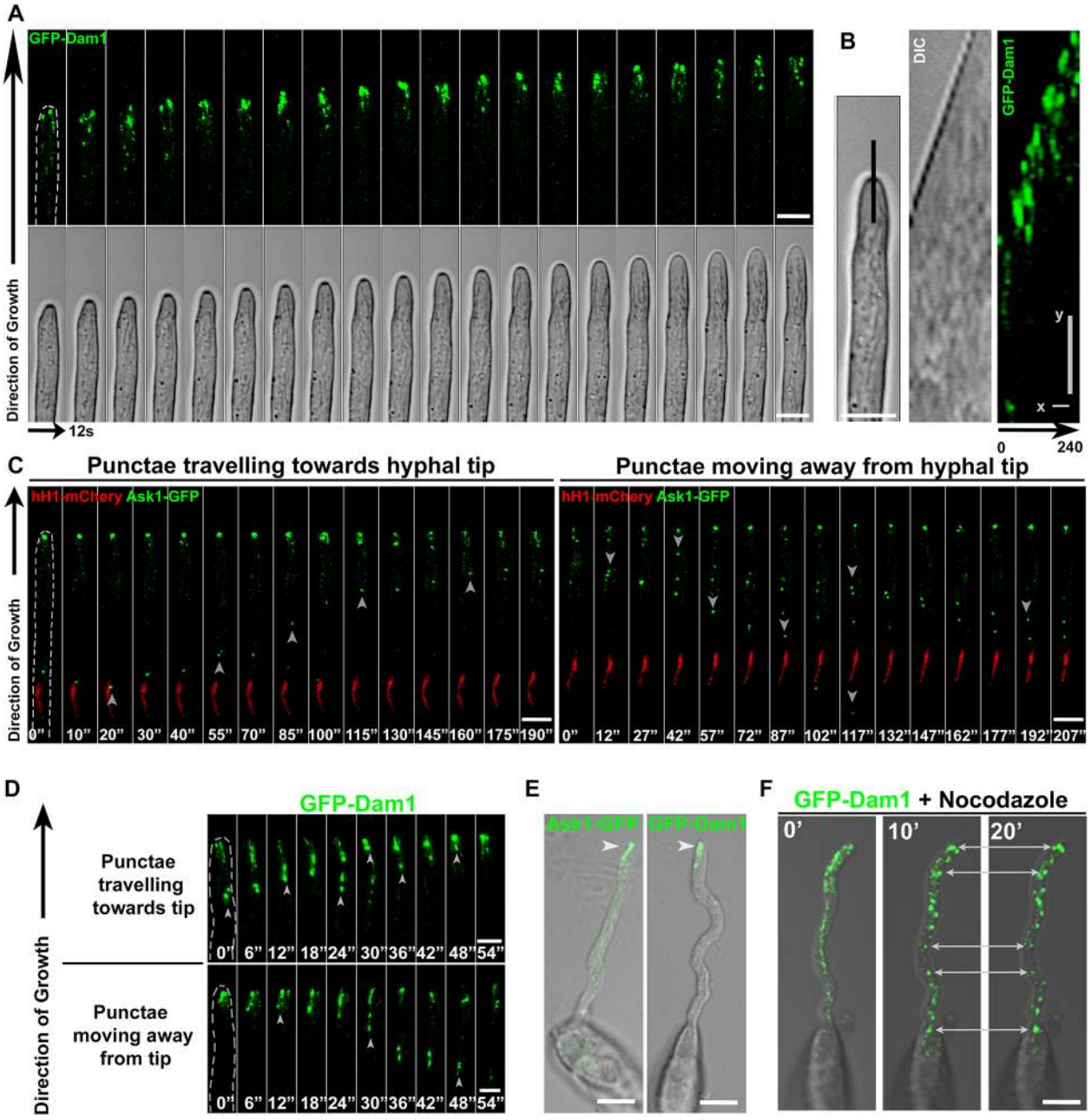

Fig. 4. DASH complex proteins localise to the hyphal tip during interphase. (A) Localisation of GFP–Dam1 at the hyphal tip during vegetative growth, *n*=30. Hyphal borders are shown with dashed lines. Scale bars: 5 µm. (B) Kymographs of time-lapse images of GFP–Dam1 shown in A. Kymographs are plotted along the black line marked on the hyphal tip in the left-hand panel for 240 s. Scale bars: *x*=48 s, *y*=1.5 µm. (C) Oscillation of Ask1–GFP from vegetative hyphal tip during interphase, *n*=20. Numbers indicate time in seconds. Hypha is outlined with dashed lines. Arrowheads mark the Ask1–GFP punctae moving towards or away from the tip. Scale bars: 5 µm. (D) Back-and-forth movement of GFP–Dam1 towards vegetative hyphal tip, *n*=10. Numbers indicate time in seconds. Hyphae are outlined with dashed lines. Arrowheads mark the GFP–Dam1 punctae moving towards or away from the tip. Scale bars: 3 µm. (E) Ask1–GFP and GFP–Dam1 localise in the form of dynamic punctae to the germ tube tip during polarised growth under pathogenic development on a hydrophobic surface, *n*=25. Arrowheads mark Ask1–GFP or GFP–Dam1 at the germ tube tip. Scale bars: 10 µm. (F) Effect of nocodazole treatment on GFP–Dam1 localisation, *n*=20. Arrows mark the static large aggregates of Ask–GFP or GFP–Dam1 all along the germ tube post-nocodazole treatment. Arrows mark the static large aggregates of GFP–Dam1 all along the germ tube post-nocodazole treatment. Scale bar: 5 µm.

disease lesions 5 days post-inoculation (dpi), the mutant showed fewer and smaller spots and lesions (Fig. 7F). Thus, our results show that *Magnaporthe* Dam1 is involved in differentiation of the infection structure and plays an important role in host invasion.

Taken together, our results highlight the importance of the dynamics of outer kinetochore proteins in proper chromosome segregation and polarised growth, crucial for asexual and pathogenic development in *M. oryzae*.

DISCUSSION

A key difference between fungal and metazoan kinetochores is the DASH complex that connects the inner kinetochore to the spindle MTs in fungi. The heterodecameric Dam1 complex is essential for survival in budding yeasts but not in fission yeast. A recent review suggests that in the filamentous fungus *Neurospora crassa*, not all Dam1 complex members may be essential (Freitag, 2017), indicating structural and functional differences in the outer

Journal of Cell Science (2019) 132, jcs224147. doi:10.1242/jcs.224147

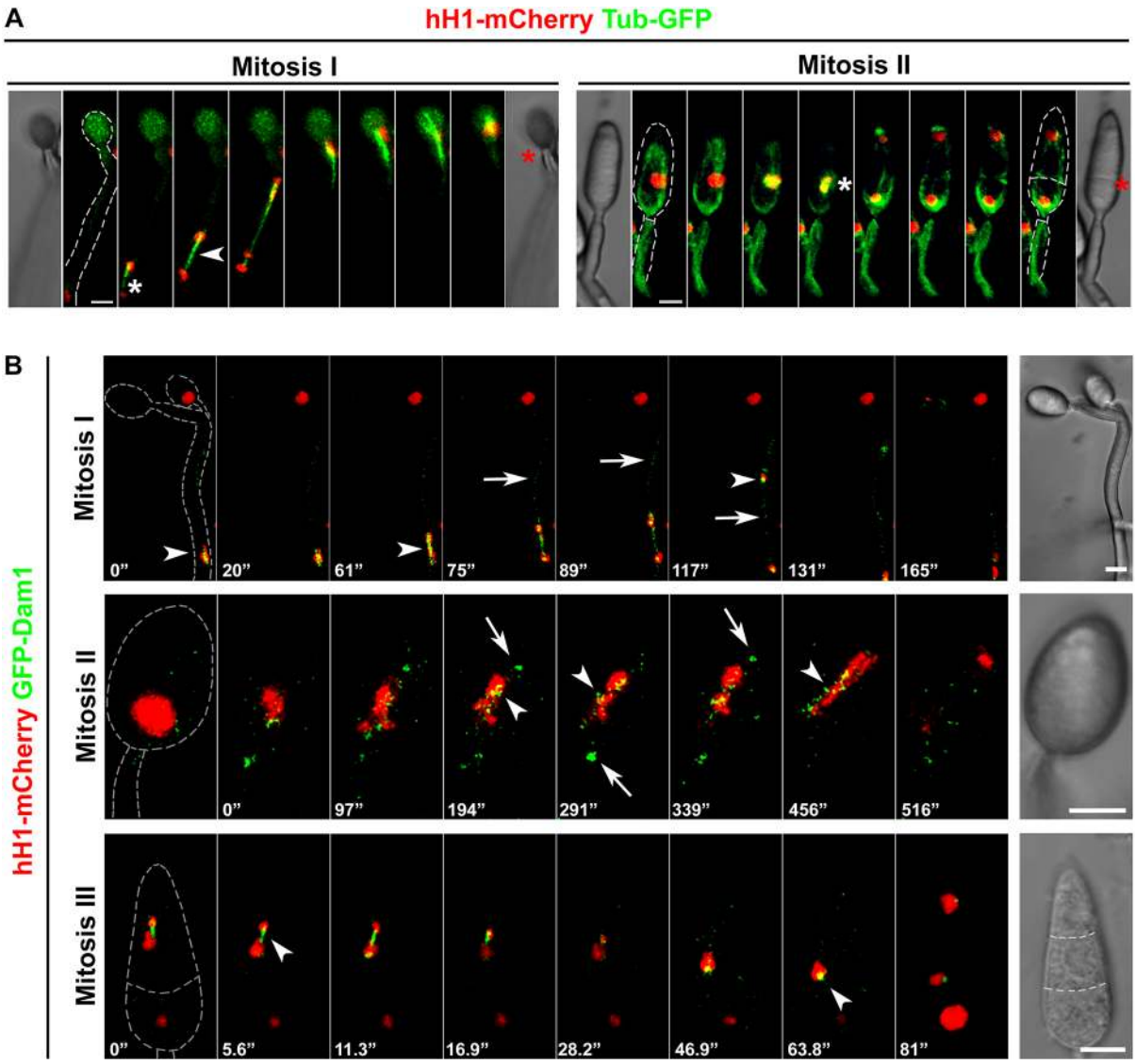

Fig. 5. Conidium development is marked by three distinct rounds of mitosis. (A) Dynamics of Tub–GFP-marked MTs or spindle, and hH1–mCherry-marked nuclear division during mitosis in the developing conidium, *n*=3. Mitosis I is observed in the stalk of the incipient conidium. Arrowhead marks the spindle, white asterisks indicate the site of mitosis, red asterisks denote the site of cytokinesis. Scale bars: 5 µm. (B) Localisation of GFP–Dam1 during three successive rounds of mitosis in the developing conidium, *n*=3. Numbers indicate time in seconds. Fungal structures are shown with dashed grey outlines. Arrowheads depict nuclear-associated GFP–Dam1, arrows indicate additional non-nuclear GFP–Dam1 spots. Scale bars: 5 µm.

kinetochore of filamentous fungi compared to that of yeasts. In budding yeasts, whether the DASH complex (also known as the Dam1 complex) is required for viability is dependent on the number of MTs attached to the kinetochore (Burrack et al., 2011; Thakur and Sanyal, 2011). However, the relationship between viability, the DASH complex and the number of MTs is not clear in filamentous fungi, where single kinetochore–MT attachment studies are currently lacking. Here, we show that the key members of the DASH complex, Dam1 and Ask1, like the previously studied *M. oryzae* Duo1 homolog, MoDuo1 (MGG_02484) (Peng et al., 2011), are not individually essential in *M. oryzae*, suggesting that more than one MT probably binds to a kinetochore in the blast fungus, or that other unknown protein interactions stabilise this kinetochore–MT attachment. The fact that we were able to generate deletion mutants of *DAM1* and *ASK1* implies that Dam1 and Ask1 are not essential for viability in *Magnaporthe*. However, although there is no complete cell cycle arrest and loss of viability in all cells within the culture, it is likely that only a fraction of cells progressed further. This was not obvious during multicellular hyphal growth but became particularly evident during conidiation and appressorium formation. Furthermore, taking into account the greatly reduced capacity of the *dam1*Δ strain to form conidia and subsequently appressoria that are able to establish infection in hosts, the net capacity for successfully infecting host plants is two orders of magnitude lower than that of the WT. A feature that differs within yeasts and from metazoan kinetochores is the timing of assembly and interdependence of middle and outer kinetochore proteins. The basidiomycete *Cryptococcus neoformans* shows ordered assembly where DASH complex proteins Dad1 and Dad2 are assembled after middle kinetochore protein Mtw1 and released before it (Kozubowski et al., 2013). In *S. cerevisiae* the Dam1 complex is associated with the kinetochore throughout the cell cycle, while all *S. pombe* DASH proteins except for Dad1 are recruited to the kinetochore during mitosis. In *M. oryzae* we found that, while Dam1 and Ask1 localised to the nucleus only at the onset of mitosis and persisted there through chromosome segregation and nuclear

Journal of Cell Science (2019) 132, jcs224147. doi:10.1242/jcs.224147

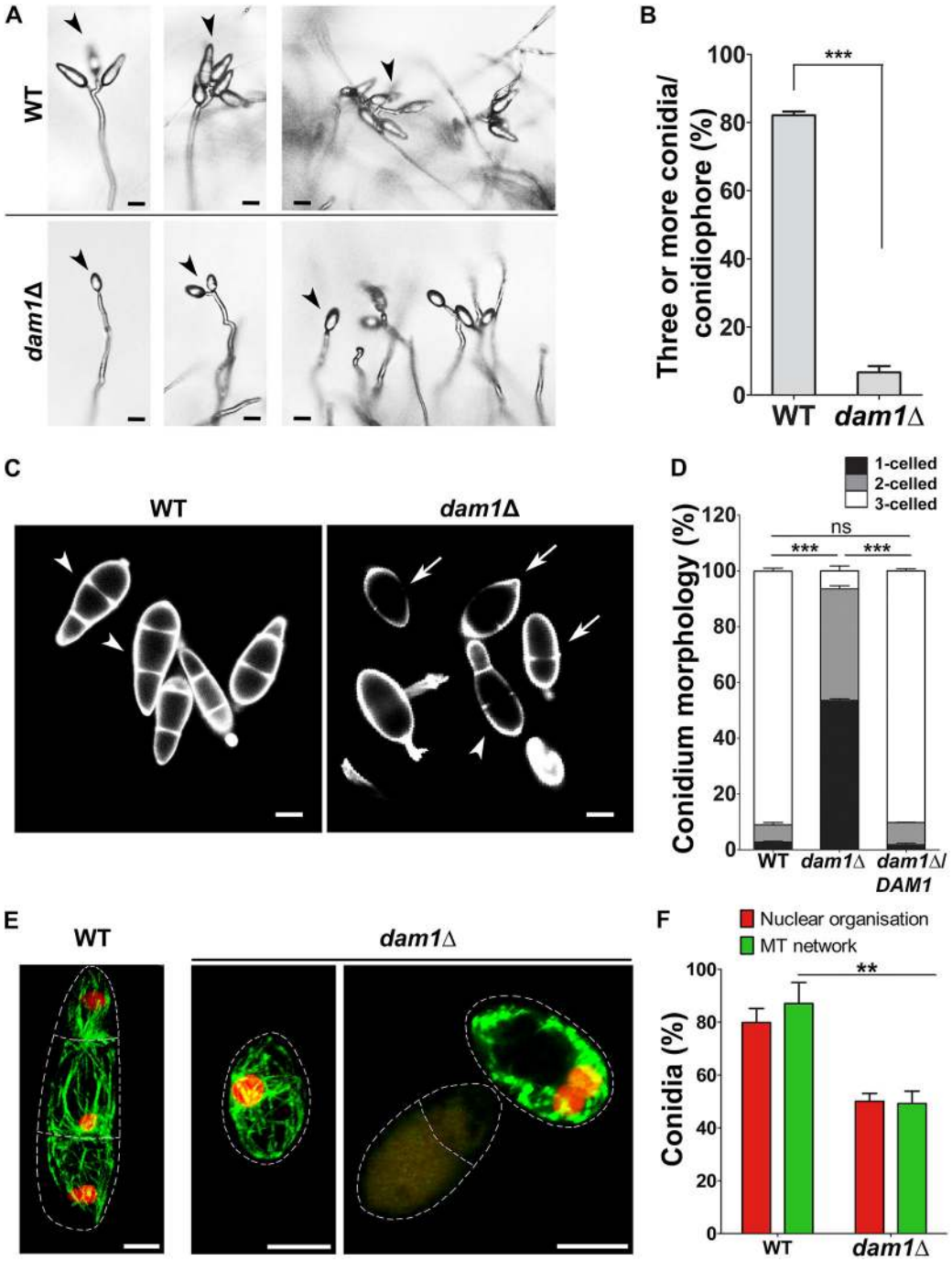

Fig. 6. Loss of Dam1 function significantly alters conidiation. (A) Difference in the conidiophore morphology and number of sympodial conidia (arrowheads) between the *dam1*Δ mutant and WT. Scale bars: 10 µm. (B) Bar chart showing mean±s.e.m. frequency of conidiophores bearing three or more conidia in the *dam1*Δ compared to the WT strain. ***P<0.0001, two-tailed *t*-test, n=300. (C) Morphology of *dam1*Δ and WT conidia stained with CFW. Arrowheads depict 3-celled conidia and arrows indicate 1- or 2-celled conidia. Scale bars: 5 µm. (D) Bar chart showing mean±s.e.m. frequency of conidia with different cell numbers (1, 2 or 3) in the WT, *dam1*Δ or *dam1*Δ/*DAM1* strain. ***P<0.0001; ns, not significantly different; two-tailed *t*-test, n=300. (E) Nuclear organisation and MT network in the WT or *dam1*Δ conidia expressing hH1–mCherry and Tub–GFP. Conidia borders are shown with dashed lines. Scale bars: 5 µm. (F) Bar chart showing mean±s.e.m. number of conidia with intact (normal) nuclear and MT organisation in the WT and *dam1*Δ mutant strains from three independent experiments. **P<0.05, two-tailed *t*-test, n=100.

migration, the MIND complex protein Mis12 appeared to be a constitutive member of the kinetochore, associating with the nucleus throughout the cell cycle at all stages of development. *S. pombe* spindle kinesins Klp5/Klp 6, and MT plus-end polymerase Mtc1 (also known as Alp14) also display metaphase-specific kinetochore localisation (Nakaseko et al., 2001; Garcia et al., 2002). Localisation of *M. oryzae* Mis12 in the form of a single spot per nucleus before mitosis indicates kinetochore clustering during interphase. These single spots of Mis12 resolved into multiple foci during mitosis, highlighting the dynamic behaviour of the kinetochore marker protein. These kinetochore dynamics in *M. oryzae* are similar to those reported in *S. pombe*, where

Journal of Cell Science (2019) 132, jcs224147. doi:10.1242/jcs.224147

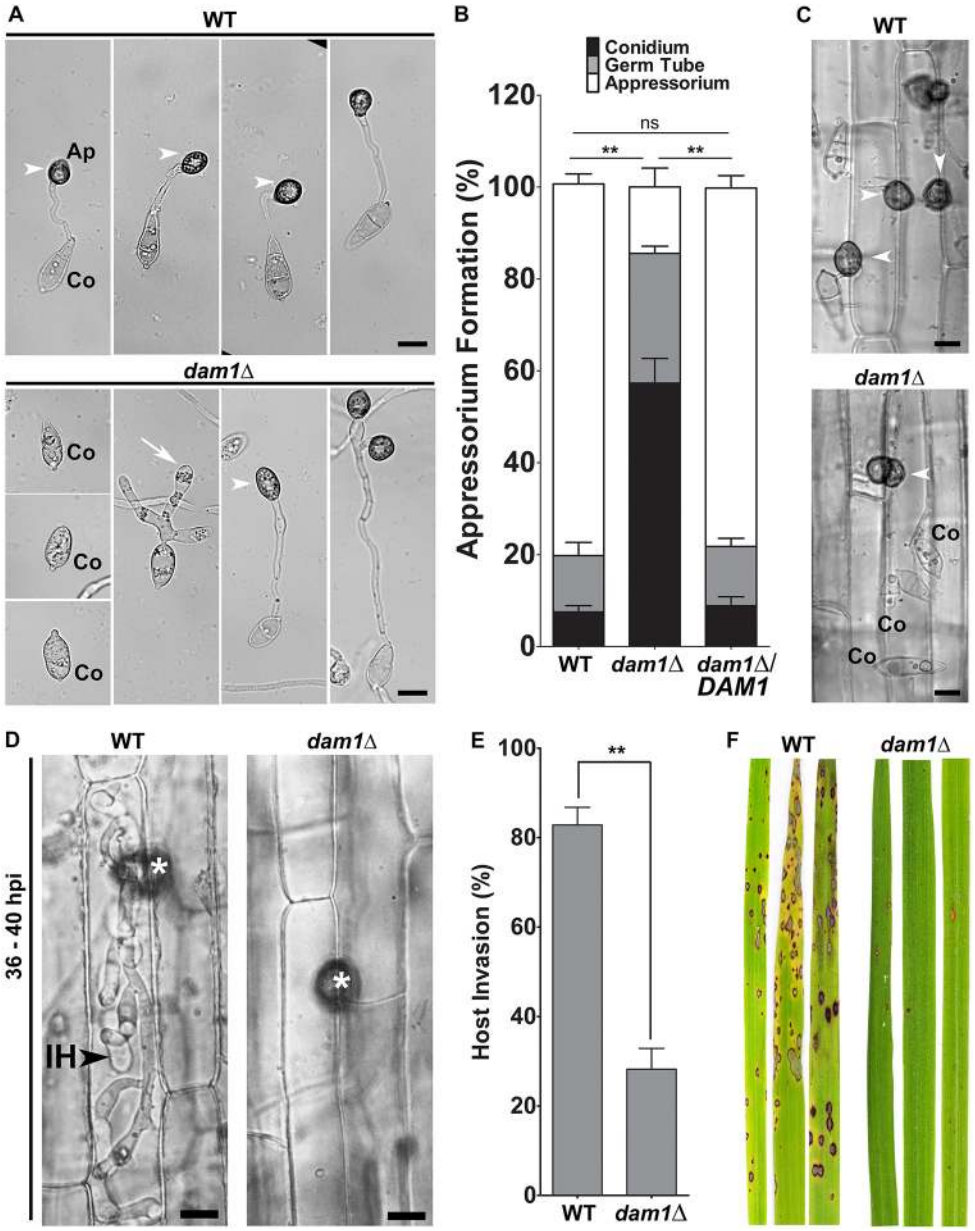

Fig. 7. Dam1 function is required for proper pathogenic development and virulence. Micrographs of pathogenic (appressorium) development on a hydrophobic surface (glass coverslips) at 24 hpi. Arrowheads depict appressoria, arrow marks an aberrant germ tube. Scale bars: 5 µm. Co, conidia. (B) Bar chart showing mean±s.e.m. frequency of appressorium formation at 24 hpi on a hydrophobic surface in the *dam1Δ* and *dam1Δ/DAM1* strain compared to the WT from three independent experiments. ***P*<0.05; ns, not significantly different; two-tailed *t*-test; *n*=150 conidia. (C) Micrographs showing appressorium formation on rice leaf sheaths at 24 hpi. Arrowheads depict appressoria. Scale bars: 10 µm. Co, conidia. (D) Micrographs showing invasion of rice leaf sheaths inoculated with the WT or *dam1Δ* conidia and observed at 36–40 hpi. Arrowhead shows invasive hyphae (IH), asterisks indicate appressoria. Scale bars: 5 µm. (E) Bar chart showing mean±s.e.m. frequency of invasive hyphae at 36–40 hpi on rice leaf sheaths in the *dam1Δ* compared to the WT strain from three independent experiments. ***P*<0.05, two-tailed *t*-test, *n*=100 appressoria. (F) Whole-plant infection assay using susceptible rice variety CO-39 and 10^5 ml^{-1} conidia of WT or *dam1Δ* strains. Leaves from inoculated plants were photographed 5 dpi. Data represent results from two independent experiments.

kinetochore de-clustering is seen in metaphase (Goshima et al., 1999). In contrast, de-clustering of kinetochore during mitosis is not visibly evident in the budding yeasts (Roy et al., 2011). Budding yeast MIND (Mis12) and NDC80 complexes show great plasticity, with many copies of proteins being added to the 'G1 configuration' of the kinetochore to form the 'anaphase configuration' kinetochore (Dhatchinamoorthy et al., 2017). Such a plastic kinetochore structure probably maintains more stable attachment during chromosome separation, while allowing correction of mis-attached chromosomes during metaphase. Whether this is the case in *M. oryzae* and can be extended to other outer kinetochore complexes in filamentous fungi will require further study. We observed that the size of the *M. oryzae* Mis12 cluster associated with the nucleus before mitosis was larger than the one observed after division (Fig. 1B), probably due to a duplicate set of kinetochores associated with each nucleus, or assembly of additional Mis12 complexes prior to mitosis. Overall, the cell cycle dynamics of DASH complex proteins and Mis12 in *M. oryzae* are more similar to those in *S. pombe* than in budding yeast or humans.

The Dam1 protein in fission yeast is involved in timely anaphase onset and lack of Dam1 leads to lagging chromosomes and sister chromatids occasionally segregating to the same pole (Sanchez-Perez et al., 2005). Along with the spindle kinesin Klp5, Dam1 is involved in chromosome biorientation. In budding yeast, the Dam1 complex proteins play an important role in maintaining spindle structure and integrity, with *DAM1* mutants showing diverse spindle defects ranging from elongated, hyperelongated, extremely short to even broken spindles (Hofmann et al., 1998; Janke et al., 2002; Cheeseman et al., 2001a,b). Similarly, mutations in budding yeast motor proteins, such as Kar3 (kinesin-14 family protein, Klp2 in *S. pombe*), Cin8, Kip1 (kinesin-5 family protein) and Kip3 (kinesin-8 family protein, Klp5/Klp6 in *S. pombe*) involved in MT stability, also display changes in spindle length (Straight et al., 1998; Zeng et al., 1999). Further, Dam1 plays a role in correct kinetochore attachments and bi-orientation in budding as well as fission yeast, lack of which leads to activation of the spindle assembly checkpoint (SAC), delaying the onset of anaphase (Janke et al., 2002; Sanchez-Perez et al., 2005; Buttrick et al., 2012). Dam1 phosphorylation by

Journal of Cell Science (2019) 132, jcs224147. doi:10.1242/jcs.224147

Aurora B kinase (also known as Ipl1) in budding yeast and Polo kinase Plo1 in *S. pombe* allows dissociation of incorrect kinetochore–MT attachments. This kinetochore is then free to be captured by a new MT until bi-orientiation of sister chromatids is sensed by tension between the two spindle poles. The *M. oryzae* Dam1 sequence also contains the Polo consensus site DTSFVD (amino acids 150–155). In *Magnaporthe*, loss of Dam1 function led to delayed anaphase onset, occasionally ending in unequal nuclear division. Such a delay was probably due to SAC activation resulting from the lack of chromosome bi-orientation in the *dam1*Δ strain of *M. oryzae*. These events of improper nuclear division and cell cycle arrest account for the reduced hyphal growth and loss of viability of conidia. Further, the *dam1*Δ mutant showed altered spindle length with some instances of collapsed spindles. Thus, *Magnaporthe* Dam1 probably plays a key role in both maintenance of spindle structure as well as bi-orientation of chromosomes.

In *M. oryzae*, differentiation of the germ tube into appressorium and the conidiophore into conidium are morphologically similar processes, requiring a switch-over from polarised to isotropic growth associated with asymmetric cell division. While the role of cell cycle checkpoints in appressorium development has been revealed, similar studies into the development of the aerial conidiophore structure have so far proved technically more challenging in *Magnaporthe*. Two different types of cytokinesis, depending on the site of septation, have been described in *M. oryzae*: 1) septation at the site of mitosis in growing vegetative hyphae, and 2) septation spatially uncoupled from mitosis during appressorium formation, where the mitosis occurs in the germ tube while the septum is placed at the neck of the newly formed appressorium (Saunders et al., 2010a,b). We observed both these types of cytokinesis during conidiation. The first septation occurred at the neck of the incipient conidium, away from the site of nuclear division occurring in the conidiophore stalk, similar to the one seen during appressorium development. The deposition of the two subsequent septa in the developing conidium occurred at the site of mitosis as seen in the case of vegetative hyphae. We further showed that nuclear association of Dam1 plays a crucial role in these three rounds of mitosis during conidial development. Conidial development was significantly impaired in the *dam1*Δ mutant with altered septation, most likely resulting from aberrant microtubular dynamics and/or unequal nuclear division. Another DASH complex protein in *M. oryzae*, MoDuo1, has previously been implicated in proper conidiation; however, its precise role in the process remains elusive (Peng et al., 2011). Defective septation, similar to that observed in this study during conidial development in the *dam1*Δ mutant, has also been found in the absence of function of the *M. oryzae* Tea4 homolog, MoTea4 (MGG_06439), which is mainly involved in cell polarity (Patkar et al., 2010), suggesting a non-canonical role for *M. oryzae* Dam1 and Ask1 during polarised growth. Indeed, loss of Dam1 function led to defects in hyphal morphology and patterning, with the *dam1*Δ mutant exhibiting excessive branching, irregular hyphal diameter and altered cell size. In *M. oryzae*, loss of Spa2, a component of the spindle pole body, also results in excessive branching (Li et al., 2014). Interestingly, independent of the role of Dam1 as a kinetochore protein, dynamic punctae of varying sizes were seen at the hyphal tip under polarised growth during interphase. In *Aspergillus nidulans* hyphal tips, most MTs are arranged with their plus-ends directed towards the tip (Konzack et al., 2005), and kinesin KipA moves along MTs towards the hyphal tip and accumulates at the MT plus-ends. Loss of KipA affects polarity maintenance through changes in the MT–cortex interaction during hyphal growth (Konzack et al., 2005). Taking into account that DASH complex proteins are plus-end MT-binding proteins in yeasts, the tip signal in *M. oryzae* is probably from Dam1 associated with the MTs at the plus ends, driving hyphal extension. The localisation pattern of Dam1 and Ask1 in *M. oryzae* is also similar to the kinesin KipA and MT polymerase AlpA in *Aspergillus nidulans*. The Dam1 or Ask1 punctae at the tips were highly dynamic, oscillating between the hyphal end and nucleus, suggesting a possible role in scanning until the nucleus is ready to undergo division. In *S. pombe*, Dam1 punctae move along the cytoplasmic MTs, occasionally merging into larger oligomers, or crossing over to neighbouring MT tracks (Gao et al., 2010). *S. pombe* Dam1 also alters the rate of depolymerisation of spindle as well as cytoplasmic MTs. It is likely that in *M. oryzae*, Dam1 is associated with the cytoplasmic MTs during interphase. Indeed, the dynamic Dam1 punctae largely disappeared during interphase upon treatment with the MT-destabilising agent nocodazole. It will also be interesting to see whether Dam1 and Ask1 proteins migrate as a complex to the tip or travel individually to assemble into a complex at the hyphal tip. We have seen that the dynamic localisation pattern of GFP–Dam1 at the hyphal tip is altered in the *ask1*Δ mutant, with relatively fewer and sluggish punctae, suggesting that the movement of Dam1 may depend on Ask1. A dual-tagged strain will provide a better understanding of the association of Dam1 and Ask1 during back-and-forth movement and tip localisation. It would be worth studying interactions, if any, between *M. oryzae* Dam1 and other MT-associated proteins and motor proteins, and their role in regulating the MT network, especially during interphase.

Penetration peg formation during host invasion involves polarised growth and one round of mitosis in the appressorium, to contribute a nucleus to the emerging invasive hyphae (Jenkinson et al., 2017). Although defects were observed in host penetration and colonisation in the *dam1*Δ mutant, it is not clear whether the defects resulted only from aberrant mitotic progression, or a combined effect of impaired penetration peg polarity and development. Determining Dam1 localisation patterns during this early host penetration stage will allow a better understanding of its role in pathogenicity. Here, we propose that in addition to its role in chromosome segregation, Dam1 plays a significant role in polarised growth. To study whether such a non-canonical function is conserved in other filamentous fungi, further characterisation of respective kinetochores would be required. Since model fungi such as *N. crassa* and *Aspergillus*, unlike *Magnaporthe*, are multi-nucleate, detailed studies on DASH complex proteins in these fungi might shed light on some interesting and novel mechanisms underlying KT dynamics.

In conclusion, the DASH complex proteins Dam1 and Ask1, though not essential for viability, have important roles to play in cell cycle progression during fungal development. Given its importance in pathogenesis and specificity to fungi, Dam1 makes a potential target for the development of novel antifungal strategies.

MATERIALS AND METHODS

Fungal strains, culture and transformation

Magnaporthe oryzae B157 strain (MTCC accession number 12236), belonging to the international race IC9 was previously isolated in our laboratory from infected rice leaves (Kachroo et al., 1994). The fungus was grown and maintained on prune agar (PA). Liquid complete medium (CM) was used to grow biomass for DNA isolation etc. Vegetative growth of the deletion mutants was measured in terms of colony diameter on PA. For conidiation, cultures were grown on PA for 3 days in the dark and then kept under constant light until harvesting. For harvesting conidia, the protocol followed was as described (Patkar et al., 2012). Quantification of conidia was done using a haemocytometer. For gene tagging and deletion, plasmids

were transformed into *M. oryzae* by protoplast transformation or *Agrobacterium tumefaciens* mediated transformation (ATMT) (Mullins et al., 2001). The transformants were selected on yeast-extract glucose agar (YEGA) with 300 µg ml^{-1} Zeocin or 300 µg ml^{-1} hygromycin or basal medium with 100 µg ml^{-1} chlorimuron ethyl or 50 µg ml^{-1} glufosinate ammonium. The selected transformants were screened by locus-specific PCR and microscopy. Single site-specific integration was confirmed by Southern hybridisation.

Plasmid construction for tagging of genes

Ask1 and Dam1 were tagged with GFP using marker fusion tagging by targeted replacement of the native locus with the GFP-tagged Dam1 construct (Lai et al., 2010). For N-terminal tagging of Dam1 (Fig. S5A,B), the *DAM1* promoter was amplified using primers Dam1-Pro-F/Dam1-Pro-R from B157 genomic DNA and cloned into p718 at EcoRI/SpeI restriction sites to obtain p718-Dam1Pro. The 1052bp *DAM1* ORF and 3′-UTR fragment was amplified using primers Dam1-ORF-F/Dam1-3UTR-R and cloned in p718-Dam1Pro in frame with *BAR–GFP* to give p718-GFPDam1. For C-terminal tagging of Ask1 (Fig. S5C,D), the 3′-end of ASK1 ORF was amplified using primers Ask1tagcdsF-ER1/Ask1tagcdsR-Spe1 from B157 genomic DNA and cloned into p718 at EcoRI/SpeI restriction sites to obtain p718-Ask1Up. The ASK1 3′-UTR was amplified using primers Ask1stop3UTRF-Hpa1/Ask13UTRR-KpnI and cloned into p718-Ask1Up to give p718-Ask1GFP. For C-terminal tagging of Mis12 (Fig. S5E,F), the Mis123′-UTR was amplified using primers Mis123UTRF-Pst1/Mis123UTRR-H3 from B157 gDNA and cloned into pFGl347 at the PstI/HindIII restriction sites to obtain pFGL347-Mis123′UTR. The last 1 kb of the MIS12 ORF was amplified using primers Mis12orf1kbF-E1/Mis12orfR. This fragment was fused with the GFP ORF (amplified using VenusF-Mis12OH/VenusR-KpnI) by PCR. The fusion product was cloned into pFGL347-Mis123′UTR at EcoRI/KpnI restriction sites to give pFGL347-Mis12GFP. All primers used in the study are listed in Table S2. All clones were confirmed by restriction enzyme digestion. PCR was carried out using XT-5 polymerase (Genei Laboratories Pvt. Ltd.) and restriction digestion was done using Fast Digest enzymes (Thermo Fisher Scientific). To mark the *M. oryzae* nucleus, hH1–mCherry-tagged B157 strain was generated using the sulfonylurea resistance reconstitution (SRR) vector pFGL959-hH1mCherry, a modified version of the pFGL959 plasmid (Yang and Naqvi, 2014) (Fig. S6A). The plasmid carrying a hH1–mCherry expression cassette (*ccg1* promoter: hH1–mCherry) was moved into wild-type *M. oryzae* strain B157 by *Agrobacterium tumefaciens*-mediated transformation (ATMT). The tagged strain was confirmed by PCR, fluorescence microscopy and Southern hybridisation (Fig. S6C). The β-tubulin:sGFP tagging construct was derived from pMF309 (obtained from Michael Freitag, Ohio State University, Columbus, USA) (Fig. S6B). The β-tubulin:sGFP cassette with the *ccg1* promoter was digested from pMF309 with HpaI/SalI and ligated to KS-HPT at HpaI/XhoI restriction sites to generate KS-HPT-β-tubulin:sGFP. This KS-HPT-β-tubulin:sGFP vector was moved into the hH1:mCherry-tagged B157 strain by protoplast transformation and transformants were selected on hygromycin and confirmed by PCR and Southern hybridisation (Fig. S6D,E). The Ask1–GFP, GFP–Dam1 and Mis12–GFP constructs were transformed into the H1–mCherry tagged strain by ATMT. Targeted replacement of native locus and single copy integration was confirmed by Southern hybridisation (Fig. S5B,D,F). All tagged strains were assessed for their virulence using drop inoculation of conidial suspension on detached barley leaves and were found to be pathogenic (Fig. S5G, Fig. S6F). Details of all strains generated in the study are provided in Table S3. All molecular biology procedures were followed as described previously (Sambrook et al., 1989).

Construction of plasmids for deletion of genes

The *DAM1* deletion cassette (Fig. S7A) was generated by double-joint PCR. The 972 bp upstream and 530 bp downstream flanking regions were amplified from B157 genomic DNA and fused with the 1.24 kb Zeocin resistance cassette by double-joint PCR. This construct was cloned into an ATMT-based plasmid. For ASK1 deletion (Fig. S7D), the 1080 bp 5′- and 889 bp 3′-flanking regions of the *ASK1* ORF were cloned upstream and downstream of the hygromycin resistance cassette. The deletion transformants were screened by locus-specific PCR (Fig. S7B,E). Correct deletion of the *DAM1* and *ASK1* ORF was confirmed by Southern hybridisation (Fig. S7C,F).

Complementation of *dam1*Δ strain

The N-terminal GFP–Dam1 construct developed earlier for localisation studies was used for complementation of the *dam1*Δ mutant (Fig. S4A). The construct was transferred into the *dam1*Δ strain by ATMT. Bialaphos-resistant transformants were screened by PCR (Fig. S4B). Southern hybridisation was used to confirm integration of a single copy of the *DAM1* construct (Fig. S4C). Transformants with a single *DAM1* copy were selected for phenotypic characterisation. The complementation transformants were analysed for hyphal growth (colony diameter), conidiation and appressorial development.

Microscopy

Bright-field and epifluorescence microscopy were performed on an Olympus BX51 (Olympus) or Nikon Eclipse80i (Nikon) microscope with 40× extra-long working distance (ELWD) or 100×/1.40 oil immersion objectives using the appropriate filter set. Sub-cellular localisation was studied by laser scanning microscopy on a LSM 700 inverted confocal microscope (Carl Zeiss Inc.). The objectives used were either an EC Plan-Neofluar 40×/1.30 or a Plan-Apochromat 63×/1.40 oil immersion lens. GFP and mCherry were imaged with the 488 nm and 555 nm laser, respectively. For live-cell imaging, fungal cultures were inoculated on glass-bottom Petri dishes. To study protein dynamics, fungal structures were captured as a time series of *z*-stack images. The images were acquired through ZEN 2010 software with the Zeiss AxioCam MR camera and processed and analysed using ImageJ (https://imagej.nih.gov/ij/download.html) and Adobe Photoshop CS6 software. 3 µg ml^{-1} Calcofluor White (Whitener 28, Sigma-Aldrich) was used to stain the cell wall and septa of conidia and vegetative hyphae. To study hyphal morphology, methods described for studying *Neurospora* hyphal growth and branching (Riquelme et al., 1998; Riquleme and Bartnicki-Garcia, 2004) were adapted for *M. oryzae*. The cultures were grown in 35 mm plates with a 3–5 mm-thick basal medium until the colony grew to a size of 2 cm. The growing edge of the colony was then observed using a 40× or 100× objective. The hyphal lengths and angles were measured using ImageJ. For fluorescence microscopy, the cultures were inoculated in plates with 2 mm thick medium. To examine the effects of the MT inhibitor nocodazole on GFP–Dam1 dynamics in germ tubes, germinating conidia were treated with 0.5 µM nocodazole for 15 min and images were taken every 5 min.

Pathogenicity assays

For appressorial assays, *M. oryzae* conidia were harvested from 10-day-old prune agar cultures. Aliquots (20 µl) of conidial suspensions (5×10^4 conidia ml^{-1} in sterile water with streptomycin) were applied on hydrophobic glass coverslips and incubated under humid conditions at room temperature. Conidial germination and appressorium formation were examined 24 h post-inoculation (hpi). The percentage of appressoria formed was calculated. For penetration assays, rice leaf sheath inoculation assays were performed with conidial suspensions as described (Kankanala et al., 2007) and assessed 36–40 hpi. Penetration pegs and infection hyphae were detected by microscopy. For detached leaf assay, 8–12-day-old barley leaves were inoculated with three drops of 10µl each of conidial suspension in 0.2% gelatine. The disease outcome was recorded 5 days post-inoculation. For *in-planta* infection assays, susceptible rice CO-39 seedlings were sprayed with 10^5 ml^{-1} of wild-type *M. oryzae* and mutant conidia in 0.2% gelatine and disease symptoms were recorded 5 dpi.

Acknowledgements

We thank the Bharat Chattoo Genome Research Centre Group for useful discussions and suggestions on the manuscript. We thank Kaustuv Sanyal (Jawaharlal Nehru Centre for Advanced Scientific Research, India) for valuable and constructive discussions. We thank Naweed Naqvi (Temasek Lifesciences Laboratory, Singapore) for sharing backbone vectors used to develop gene deletion and tagging constructs in the study. We are grateful to Michael Freitag

(Ohio State University, USA) for sharing the pMF309 plasmid used to develop the tubulin–GFP tagging construct. We acknowledge late Prof. Bharat B. Chattoo who encouraged us to take up this work and made it possible with the infrastructure and facilities he established at the Bharat Chattoo Genome Research Centre.

Competing interests
The authors declare no competing or financial interests.

Author contributions
Conceptualization: H.S., R.P., J.M.; Methodology: H.S., R.P., J.M.; Validation: H.S., K.R., H.A.; Formal analysis: H.S.; Investigation: H.S., K.R., H.A.; Resources: R.P., J.M.; Writing - original draft: H.S.; Writing - review & editing: H.S., R.P., J.M.; Visualization: H.S., R.P., J.M.; Supervision: R.P., J.M.; Project administration: R.P., J.M.; Funding acquisition: H.S., R.P., J.M.

Funding
The work was supported by a Shyama Prasad Mukherjee Fellowship from the Council of Scientific and Industrial Research, India to H.S. [SPM-09/114(0129)/2012-EMR-I] and Ramalingaswami Re-Entry Fellowship from the Department of Biotechnology, Ministry of Science and Technology to R.P. (BT/RLF/Re-entry/32/2014).

Supplementary information
Supplementary information available online at
http://jcs.biologists.org/lookup/doi/10.1242/jcs.224147.supplemental

References
Burrack, L. S., Applen, S. E. and Berman, J. (2011). The requirement for the Dam1 complex is dependent upon the number of kinetochore proteins and microtubules. *Curr. Biol.* **21**, 889-896. doi:10.1016/j.cub.2011.04.002

Buttrick, G. J., Lancaster, T. C., Meadows, J. C. and Millar, J. B. A. (2012). Plo1 phosphorylates Dam1 to promote chromosome bi-orientation in fission yeast. *J. Cell Sci.* **125**, 1645-1651. doi:10.1242/jcs.096826

Cheeseman, I. M., Brew, C., Wolyniak, M., Desai, A., Anderson, S., Muster, N., Yates, J. R., Huffaker, T. C., Drubin, D. G. and Barnes, G. (2001a). Implication of a novel multiprotein Dam1p complex in outer kinetochore function. *J. Cell Biol.* **155**, 1137-1146. doi:10.1083/jcb.200109063

Cheeseman, I. M., Enquist-Newman, M., Muller-Reichert, T., Drubin, D. G. and Barnes, G. (2001b) Mitotic spindle integrity and kinetochore function are linked by the Duo1p/Dam1p complex. *J. Cell Biol.* **152**, 197-212. doi:10.1083/jcb.152.1.197

Dhatchinamoorthy, K., Shivaraju, M., Lange, J. J., Rubinstein, B., Unruh, J. R., Slaughter, B. D. and Gerton, J. L. (2017). Structural plasticity of the living kinetochore. *J. Cell Biol.* **216**, 3551-3570. doi:10.1083/jcb.201703152

Dean, R., Van Kan, J. A., Pretorius, Z. A., Hammond-Kosack, K. E., Di Pietro, A., Spanu, P. D., Rudd, J. J., Dickman, M., Kahmann, R., Ellis, J. et al. (2012). The top 10 fungal pathogens in molecular plant pathology. *Mol. Plant Pathol.* **13**, 414-430. doi:10.1111/j.1364-3703.2011.00783.x

Deng, Y. Z., Ramos-Pamplona, M. and Naqvi, N. I. (2009). Autophagy-assisted glycogen catabolism regulates asexual differentiation in *Magnaporthe oryzae*. *Autophagy* **5**, 33-43. doi:10.4161/auto.5.1.7175

Franco, A., Meadows, J. C. and Millar, J. B. A. (2007). The Dam1/DASH complex is required for the retrieval of unclustered kinetochores in fission yeast. *J. Cell Sci.* **120**, 3345-3351. doi:10.1242/jcs.013698

Freitag, M. (2017). The kinetochore interaction network (KIN) of ascomycetes. *Mycologia* **108**, 485-505. doi:10.3852/15-182

Gao, Q., Courtheoux, T., Gachet, Y., Tournier, S. and He, X. (2010). A non-ring-like form of the Dam1 complex modulates microtubule dynamics in fission yeast. *Proc. Natl. Acad. Sci. USA* **107**, 13330-13335. doi:10.1073/pnas.1004887107

Garcia, M. A., Koonrugsa, N. and Toda, T. (2002). Two kinesin-like Kin I family proteins in fission yeast regulate the establishment of metaphase and the onset of anaphase A. *Curr. Biol.* **12**, 610-621. doi:10.1016/S0960-9822(02)00761-3

Goshima, G., Saitoh, S. and Yanagida, M. (1999). Proper metaphase spindle length is determined by centromere proteins Mis12 and Mis6 required for faithful chromosome segregation. *Genes Dev.* **13**, 1664-1677. doi:10.1101/gad.13.13.1664

Hofmann, C., Cheeseman, I. M., Goode, B. L., McDonald, K. L., Barnes, G. and Drubin, D. G. (1998). Saccharomyces cerevisiae Duo1p and Dam1p, novel proteins involved in mitotic spindle function. *J. Cell Biol.* **143**, 1029-1040. doi:10.1083/jcb.143.4.1029

Janke, C., Ortiz, J., Tanaka, T. U., Lechner, J. and Schiebel, E. (2002). Four new subunits of the Dam1-Duo1 complex reveal novel functions in sister kinetochore biorientation. *EMBO J.* **21**, 181-193. doi:10.1093/emboj/21.1.181

Jenkinson, C. B., Jones, K., Zhu, J., Dorhmi, S. and Khang, C. H. (2017). The appressorium of the rice blast fungus *Magnaporthe oryzae* remains mitotically active during post-penetration hyphal growth. *Fungal Genet. Biol.* **98**, 35-38. doi:10.1016/j.fgb.2016.11.006

Jones, K., Jenkinson, C. B., Araújo, M. B., Zhu, J., Kim, R. Y., Kim, D. W. and Khang, C. H. (2016). Mitotic stopwatch for the blast fungus *Magnaporthe oryzae* during invasion of rice cells. *Fungal Genet. Biol.* **93**, 46-49. doi:10.1016/j.fgb.2016.06.002

Kachroo, P., Leong, S. A. and Chattoo, B. B. (1994). Pot2, an inverted repeat transposon from the rice blast fungus *Magnaporthe grisea*. *Mol. Gen. Genet.* **245**, 339-348. doi:10.1007/BF00290114

Kankanala, P., Czymmek, K. and Valent, B. (2007). Roles for rice membrane dynamics and plasmodesmata during biotrophic invasion by the blast fungus. *Plant Cell* **19**, 706-724. doi:10.1105/tpc.106.046300

Konzack, S., Rischitor, P. E., Enke, C. and Reinhard, F. (2005). The role of the kinesin motor KipA in microtubule organization and polarized growth of *Aspergillus nidulans*. *Mol. Biol. Cell* **16**, 497-506. doi:10.1091/mbc.e04-02-0083

Kozubowski, L., Yadav, V., Chatterjee, G., Sridhar, S., Yamaguchi, M., Kawamoto, S., Bose, I., Heitman, J. and Sanyal, K. (2013). Ordered kinetochore assembly in the human-pathogenic basidiomycetous yeast *Cryptococcus neoformans*. *MBio* **4**, e00614-e00613. doi:10.1128/mBio.00614-13

Lai, J., Ng, S. K., Liu, F. F., Patkar, R. N., Lu, Y., Chan, J. R., Suresh, A., Naqvi, N. and Jedd, G. (2010). Marker fusion tagging, a new method for production of chromosomally encoded fusion proteins. *Eukaryot. Cell* **9**, 827-830. doi:10.1128/EC.00386-09

Legal, T., Zou, J., Sochaj, A., Rappsilber, J. and Welburn, J. P. I. (2016). Molecular architecture of the Dam1 complex-microtubule interaction. *Open Biol.* **6**, 1-9. doi:10.1098/rsob.150237

Li, C., Yang, J., Zhou, W., Chen, X.-L., Huang, J.-G., Cheng, Z.-H., Zhao, W.-S., Zhang, Y. and Peng, Y.-L. (2014). A spindle pole antigen gene MoSPA2 is important for polar cell growth of vegetative hyphae and conidia, but is dispensable for pathogenicity in *Magnaporthe oryzae*. *Curr. Genet.* **60**, 255-263. doi:10.1007/s00294-014-0431-4

Liu, X., McLeod, I., Anderson, S., Yates, J. R. and He, X. (2005). Molecular analysis of kinetochore architecture in fission yeast. *EMBO J.* **24**, 2919-2930. doi:10.1038/sj.emboj.7600762

Mullins, E. D., Chen, X., Romaine, P., Raina, R., Geiser, D. M. and Kang, S. (2001). *Agrobacterium*-mediated transformation of *Fusarium oxysporum*: an efficient tool for insertional mutagenesis and gene transfer. *Phytopathology* **91**, 173-180. doi:10.1094/PHYTO.2001.91.2.173

Nakaseko, Y., Goshima, G., Morishita, J. and Yanagida, M. (2001). M phase specific kinetochore proteins in fission yeast: microtubule-associating Dis1 and Mtc1 display rapid separation and segregation during anaphase. *Curr. Biol.* **11**, 537-549. doi:10.1016/S0960-9822(01)00155-5

Ng, C. T., Deng, L., Chen, C., Lim, H. H., Shi, J., Surana, U. and Gan, L. (2019). Electron cryotomography analysis of Dam1C/DASH at the kinetochore–spindle interface *in situ*. *J. Cell Biol.* **218**, 455-473. doi:10.1083/jcb.201809088

Patkar, R. N., Suresh, A. and Naqvi, N. I. (2010). MoTea4-mediated polarized growth is essential for proper asexual development and pathogenesis in *Magnaporthe oryzae*. *Eukaryot. Cell* **9**, 1029-1038. doi:10.1128/EC.00292-09

Patkar, R. N., Ramos-Pamplona, M., Gupta, A. P., Fan, Y. and Naqvi, N. I. (2012). Mitochondrial beta-oxidation regulates organellar integrity and is necessary for conidial germination and invasive growth in *Magnaporthe oryzae*. *Mol. Microbiol.* **86**, 1345-1363. doi:10.1111/mmi.12060

Peng, H., Feng, Y., Zhu, X., Lan, X., Tang, M., Wang, J., Dong, H. and Chen, B. (2011). MoDUO1, a Duo1-like gene, is required for full virulence of the rice blast fungus *Magnaporthe oryzae*. *Curr. Genet.* **57**, 409-420. doi:10.1007/s00294-011-0355-1

Riquelme, M. and Bartnicki-Garcia, S. (2004). Key differences between lateral and apical branching in hyphae of *Neurospora crassa*. *Fung. Gen. Biol.* **41**, 842-851. doi:10.1016/j.fgb.2004.04.006

Riquelme, M., Reynaga-Peña, C. G., Gierz, G. and Bartnicki-Garcia, S. (1998). What determines growth direction in fungal hyphae? *Fung. Genet. Biol.* **24**, 101-109. doi:10.1006/fgbi.1998.1074

Roy, B., Burrack, L. S., Lone, M. A., Berman, J. and Sanyal, K. (2011). CaMtw1, a member of the evolutionarily conserved Mis12 kinetochore protein family, is required for efficient inner kinetochore assembly in the pathogenic yeast *Candida albicans*. *Mol. Microbiol.* **80**, 14-32. doi:10.1111/j.1365-2958.2011.07558.x

Sambrook, J., Fritsch, E. F. and Maniatis, T. (1989). *Molecular Cloning: A Laboratory Manual*, 2nd edn. New York: Cold Spring Harbour Laboratory Press.

Sanchez-Perez, I., Renwick, S. J., Crawley, K., Karig, I., Buck, V., Meadows, J. C., Franco-Sanchez, A., Fleig, U., Toda, T. and Millar, J. B. (2005). The DASH complex and Klp5/Klp6 kinesin coordinate bipolar chromosome attachment in fission yeast. *EMBO J.* **24**, 2931-2943. doi:10.1038/sj.emboj.7600761

Saunders, D. G. O., Aves, S. J. and Talbot, N. J. (2010a). Cell cycle-mediated regulation of plant infection by the rice blast fungus. *Plant Cell* **22**, 497-507. doi:10.1105/tpc.109.072447

Saunders, D. G. O., Dagdas, Y. F. and Talbot, N. J. (2010b). Spatial uncoupling of mitosis and cytokinesis during appressorium-mediated plant infection by the rice blast fungus *Magnaporthe oryzae*. *Plant Cell* **22**, 2417-2428. doi:10.1105/tpc.110.074492

Straight, A. F., Sedat, J. W. and Murray, A. W. (1998). Time-lapse microscopy reveals unique roles for kinesins during anaphase in budding yeast. *J. Cell Biol.* **143**, 687-694. doi:10.1083/jcb.143.3.687

Thakur, J. and Sanyal, K. (2011). The essentiality of the fungus-specific Dam1 complex is correlated with a one-kinetochore-one-microtubule interaction present throughout the cell cycle, independent of the nature of a centromere. *Eukaryot. Cell* **10**, 1295-1305. doi:10.1128/EC.05093-11

Van Hooff, J. J. E., Tromer, E., van Wijk, L. M., Snel, B. and Kops, G. J. P. L. (2017). Evolutionary dynamics of the kinetochore network as revealed by comparative genomics. *EMBO Rep.* **18**, 1559-1571. doi:10.15252/embr.201744102

Yang, F. and Naqvi, N. I. (2014). Sulfonylurea resistance reconstitution as a novel strategy for ILV2-specific integration in *Magnaporthe oryzae*. *Fungal Genet. Biol.* **68**, 71-76. doi:10.1016/j.fgb.2014.04.005

Zeng, X., Kahana, J. A., Silver, P. A., Morphew, M. K., McIntosh, J. R., Fitch, I. T., Carbon, J. and Saunders, W. S. (1999). Slk19p is a centromere protein that functions to stabilize mitotic spindles. *J. Cell Biol.* **146**, 415-425. doi:10.1083/jcb.146.2.415